Online Appendix A - Supporting Information

Index

Impact of the degree of trait matching on mating probabilities 1
Species delimitation 1
Asymptotic levels of diversity and stability of diversification patterns 3
Sensitivity analysis 4
Alternative scenarios regarding biological assumptions 6
Mutualism impact on the mating pool composition 6
Alternative P_{mut} computation 6
Symmetric constrain on the number of individual mutualistic partners 6
Relaxing the assumption of both species under disruptive selection 7
Relaxing the assumption of equal and constant population sizes 9
Literature cited in the Online Appendix 9

Impact of the degree of trait matching on mating probabilities

We used the parameter λ (see equation 4 in the main text) to describe the effect of the degree of trait matching of mutualistic interactions on the reproductive output of individuals. We assumed that λ varies between 0 and 1. If $\lambda = 1$, increasing mismatches rapdly impose great reproductive loss (fig. A1-A). Mismatched interactions are progressively less penalized under decreasing values of λ (figs. A1-B-C). As the paremeter approaches 0, interindividual variation in the reproductive impact of trait matching become uniform within the population (fig. A1-D).

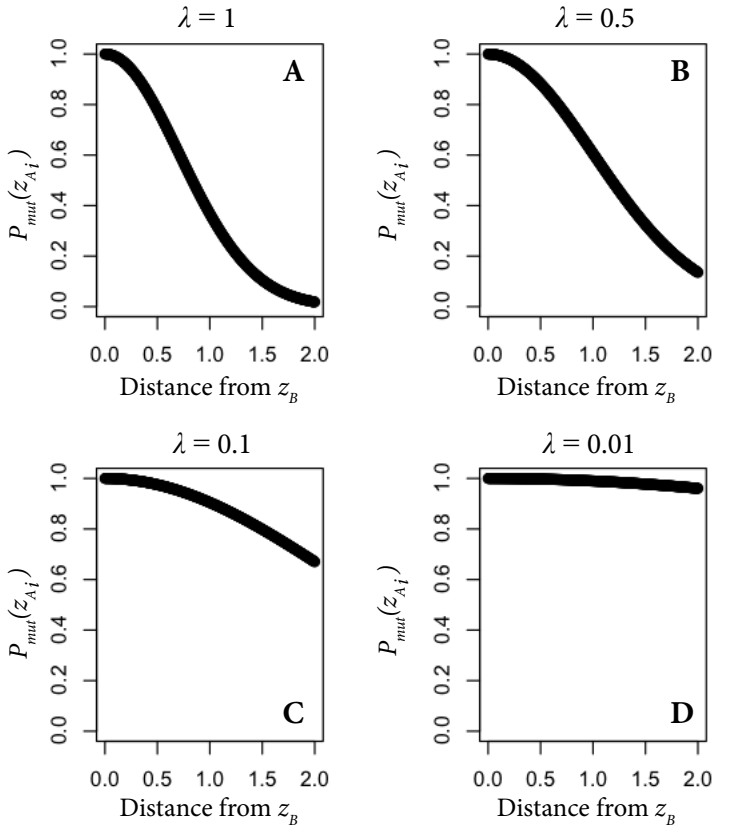

Figure A1. The reproductive outcome of mutualistic interactions, for the individuals of species *A*, $P_{mut}(z_A)$ considering a fixed value of $z_B = 1$ and different values of λ, the paramater describing the effect of the trait matching of mutualistic interactions on the individual mating probabilities.

Species delimitation

We applied a phenotypic clustering criterion (PCC) to delimit species emerging in our simulations. Phenotypic clusters are often used for species delimitation in adaptive speciation models (Doebeli and Dieckmann 2000). We built an algorithm based on the discontinuous distribution of a trait z to identify clusters defined by phenotypic discontinuities. The algorithm uses a parameter l to define the degree of discontinuity separating ecologically differentiated and reproductively isolated individuals. To test the consistency of the PCC in determining species identities in our simulations, we (i) compared species richness (S) computed under different l values to the number of lineages observed in phenotypic trajectory plots describing trait divergence through time, (ii) tracked individuals' genealogies to check for the existence of hybrids, i.e., individuals with parents belonging to different species, and (iii) examined phenotypic clusters to check if they hold individuals descending from more than one species.

With regards to (i), species richness detected by PCC is overestimated if $l < 0.1$ units of z, since individuals isolated by small phenotypic discontinuities, as those found in the extreme of each species distributions, are

classified as unique species. For example, when $l = 0.05$, the species delimitation rule recognizes up to 75 species deriving from species *A* (fig. A2, blue line), whereas the actual number of lineages is much lower (fig. A3). A better estimate for species richness within our adaptive diversification model is found when $0.1 \leq l \leq 0.2$. Values of $l >> 0.2$ underestimate species richness since ecologically specialized and reproductively isolated clusters are merged within the same species (fig. A2, black line). When $l = 0.1$, even incipient divergence between clusters are computed in the richness count (fig. A3-B), whereas $l = 0.2$ provides a more accurate approximation for the number of lineages observed in phenotypic trajectory plots (figs. A3-B, A3-D). Based on these results, we chose a value of $l = 0.2$ for the species delimitation parameter used in our species richness analyses. With regards to (ii), phenotypic clusters emerging in our adaptive diversification model can be interpreted as reproductively isolated units, since 100% of individuals had both parents belonging to the same cluster/species (n = 60,000 individuals sampled during 100 time steps uniformly distributed through 10,000 generations, l = 0.2). Therefore, each phenotypic cluster results from assortative mating within a small number of genealogically linked individuals (families)

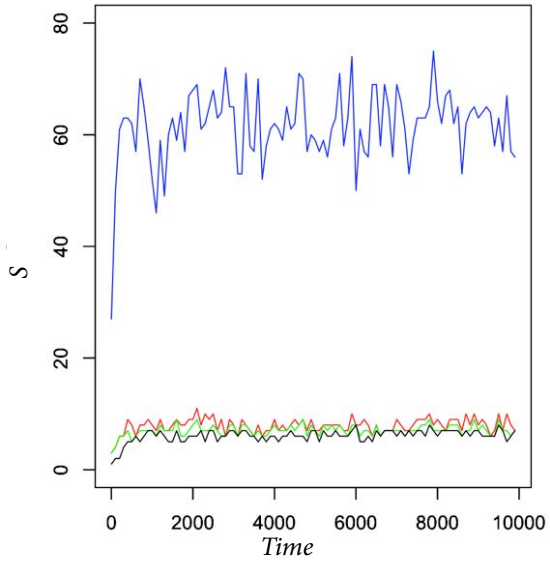

Figure A2. Temporal variation in species richness (*S*) according to the limiting parameter, *l*, used in the phenotypic clustering criterion (PCC). *S* is the sum of clades derived from species *A* and *B* emerging in simulations of adaptive diversification. Lines describe different values of *l*, which defines the phenotypic discontinuity determining species borders. Blue, $l = 0.05$; red, $l = 0.1$; green, $l = 0.2$; black, $l = 0.4$. Same parameters as those of figure 1 (see main text) through 10,000 time steps.

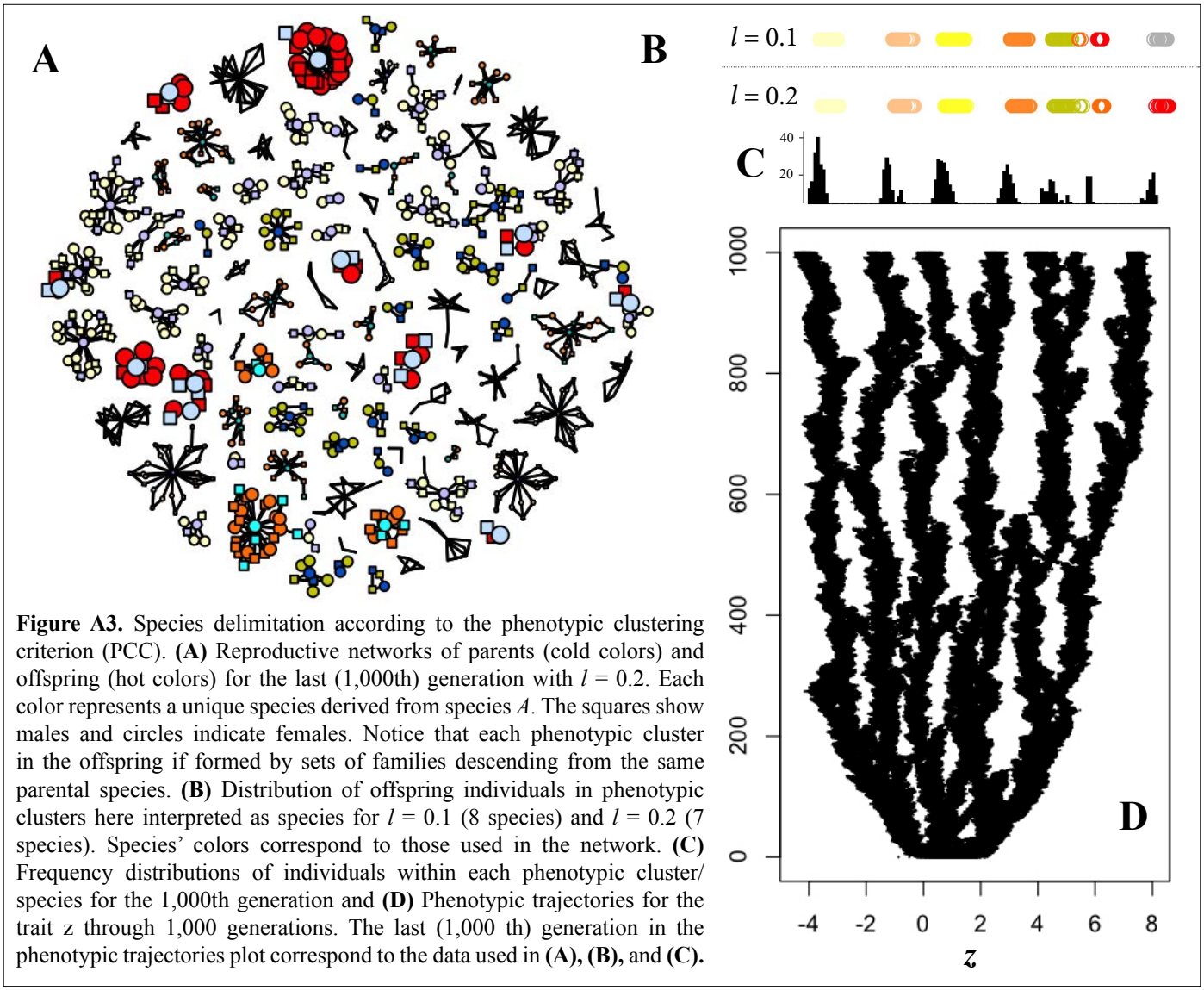

Figure A3. Species delimitation according to the phenotypic clustering criterion (PCC). **(A)** Reproductive networks of parents (cold colors) and offspring (hot colors) for the last (1,000th) generation with $l = 0.2$. Each color represents a unique species derived from species *A*. The squares show males and circles indicate females. Notice that each phenotypic cluster in the offspring if formed by sets of families descending from the same parental species. **(B)** Distribution of offspring individuals in phenotypic clusters here interpreted as species for $l = 0.1$ (8 species) and $l = 0.2$ (7 species). Species' colors correspond to those used in the network. **(C)** Frequency distributions of individuals within each phenotypic cluster/ species for the 1,000th generation and **(D)** Phenotypic trajectories for the trait z through 1,000 generations. The last (1,000 th) generation in the phenotypic trajectories plot correspond to the data used in **(A), (B),** and **(C).**

(fig. A3-A). Finally, with regards to (iii), only a small fraction of individuals within a given cluster eventually descend from multiple species. We found that 97.5 ± 10% of individuals per generation are assembled in clusters in which all organisms descend from a unique parental species (n = 60,000 sampled during 100 time steps uniformly distributed through 10,000 generations, $l = 0.2$).

Asymptotic levels of diversity and stability of diversification patterns

We used the PCC algorithm to describe the temporal variation in species richness (*S*) through 10,000 generations. The diversification patterns remained stable after 10,000 generations (Figure A4). Species

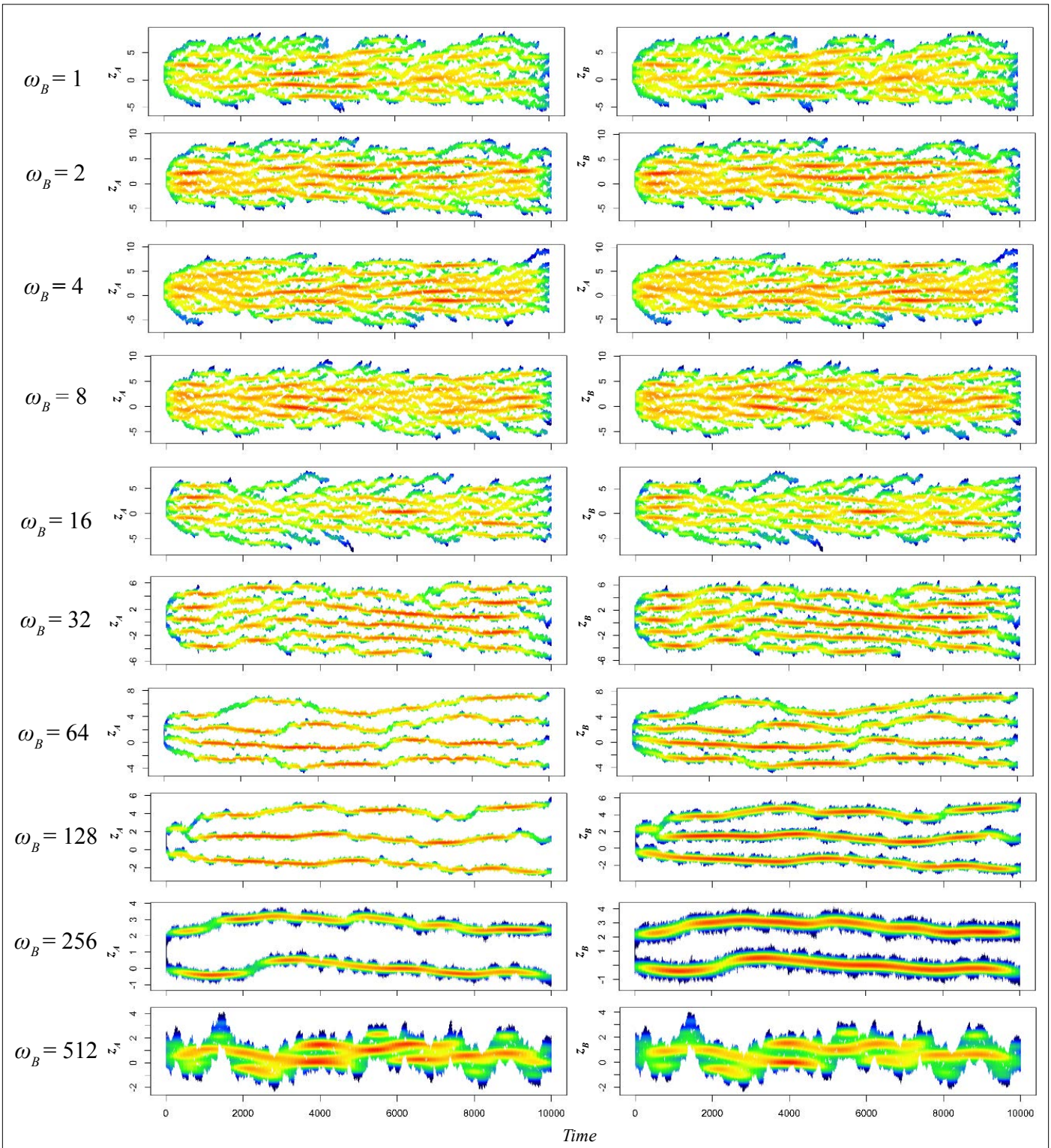

Figure A4. Phenotypic trajectories under diverse mutualism attributes through 10,000 time steps. The numbers at the left of each panel indicate the number of mutualistic partners with which each individual of species B interacted (ω_B). Other parameters are the same as in Figure 1 (see main text). Temperature colors depict density of individuals, ranging from high (hot colors) to low (cold colors).

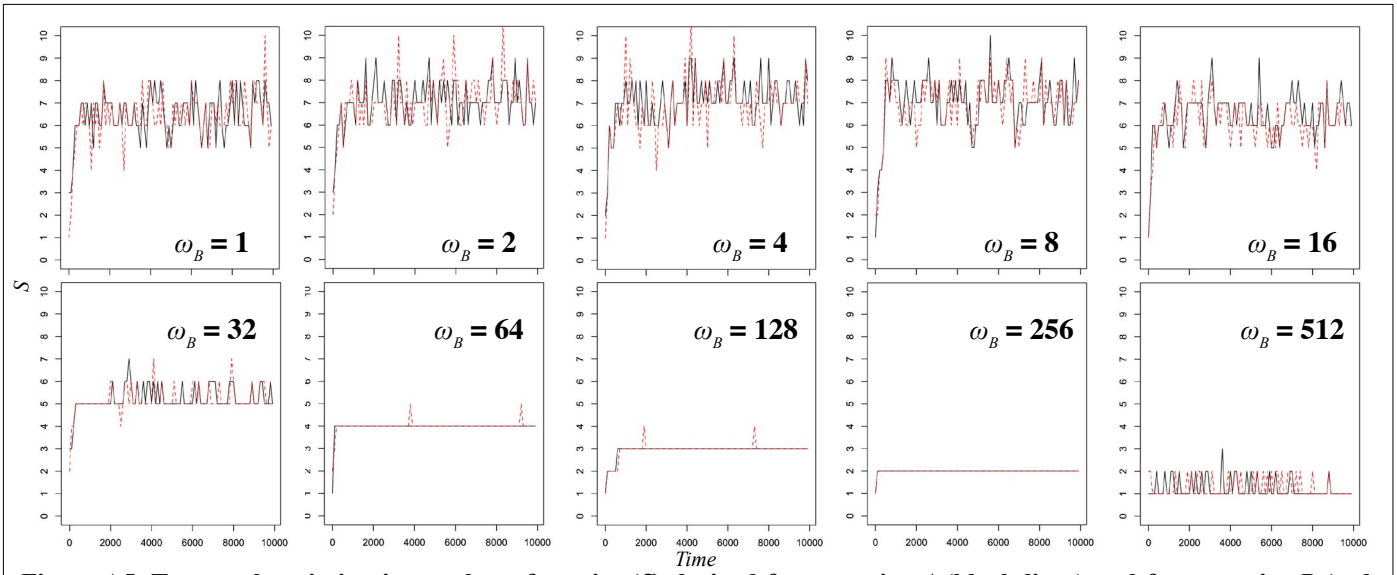

Figure A5. Temporal variation in number of species (*S*) derived from species *A* (black lines) and from species *B* (red lines) under varying ω_B. Numbers inside each panel indicate the number ω_B of mutualistic partners with which each species B individual interacted. Other parameters are the same as in Figure 1 (see the main text).

richnesses reached asymptotic levels before 1,000 time steps (fig. A5). These results are consistent under different values of the mutualism attributes (ω_B and λ). Similar asymptotic levels were also observed for another diversity measure, the Shannon-Weaver index (H'). We thus proceeded to compute species richness in simulation replicates using the number of species found by the PCC algorithm after 1,000 time steps.

Sensitivity analysis

We performed a sensitivity analysis to qualitatively describe dynamics of the coevolutionary system and associated diversification patterns throughout the parametric space. We used Latin Hypercube Sampling (LHS) to obtain parameter values covering broad areas of the parametric space with a small number of simulations. We used the R package *lhs* (Carnell 2009) to generate n by k matrices with uniformly distributed values, where $n = 20$ is the number of simulations and $k = 3$ is the number of key parameters used to model individuals' life cycle (Table A1). Values of initial trait variance, $\sigma = \sigma_A = \sigma_B$, and the strength of intraspecific competition, c, were sampled from (0,1) for each simulation. The strength of stabilizing selection, γ, was sampled from (0, 0.25), since γ values higher than 0.25 converge to a single speciation event in larger populations yield no divergence or extinction in smaller populations ($n = 320$ simulations, results not shown). We ran 20 simulations encompassing sampled parametric combinations under four population sizes ($N_A = N_B$ = 75, 150, 300, and 600), totaling 80 simulations (fig. A6).

Table A1. Parameter combinations used for sensitivity analysis. Initial trait variance ($\sigma = \sigma_A = \sigma_B$), strength of stabilizing selection (γ); and strength of intraspecific completion (c).

Sample	σ	γ	c	Sample	σ	γ	c
s1	0.58	0.00	0.74	**s11**	0.92	0.55	0.07
s2	0.76	0.08	0.56	**s12**	0.25	0.56	0.02
s3	0.61	0.10	0.62	**s13**	0.66	0.62	0.16
s4	0.73	0.15	0.54	**s14**	0.41	0.69	0.11
s5	0.05	0.24	0.39	**s15**	0.48	0.74	0.30
s6	0.19	0.28	0.97	**s16**	0.87	0.79	0.26
s7	0.01	0.31	0.49	**s17**	0.38	0.81	0.80
s8	0.32	0.36	0.21	**s18**	0.14	0.88	0.94
s9	0.52	0.40	0.79	**s19**	0.81	0.91	0.44
s10	0.30	0.46	0.88	**s20**	0.97	0.98	0.70

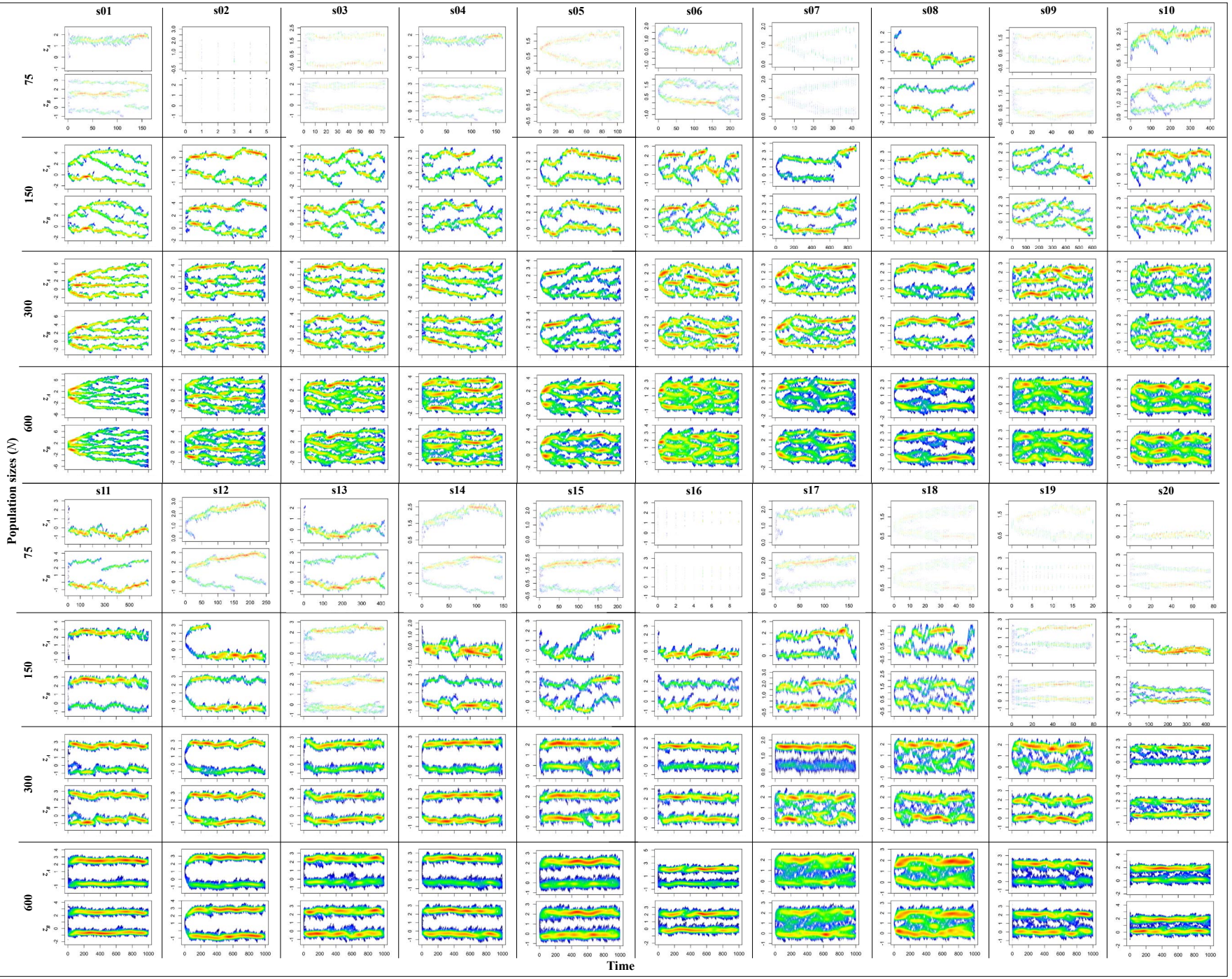

Figure A6. Phenotypic trajectories plots for both traits z_A and z_B under 20 parameter combinations (s1-s20) obtained through Latin Hypercube sampling (LHS). See Table 1 for parameters and their values. The columns present phenotypic trajectories under each parameter combination and rows show results for four population sizes (N_A = N_B = 75, 150, 300, 600). Abscissae depict the number of time steps for which each simulation ran and follow the labels in the last row, ranging from 0 to 1000, except when indicated. Simulations with different time duration ended due to species extinction. Colors represent density of individuals throughout the phenotypic space. $\omega_B = \lambda = 1$.

The highest diversification degree – a radiation-like pattern with recurrent extinctions – arises when the strength of stabilizing selection, γ, is low (< 0.1). This pattern is particularly evident in larger populations (figs. A6s1-s2). When $0.5 > \gamma > 0.1$, populations split into several stable phenotypic lineages (figs. A6s3-s10), except when the strength of intraspecific competition (c) decreases, which leads to a single branching event (fig, A6s8). When $\gamma > 0.5$, results converge to a single branching event regardless of population size (fig. A6s11-s20), except if c is low, in which case larger populations may hold polymorphisms without bifurcating (fig. A6s17-18). When $\gamma > 0.1$, most small populations (75, 150 individuals) undergo a single branching event, or branching-extinction cycles if c is near its maximum (fig. A6s6).

Alternative scenarios regarding biological assumptions

We used two interaction attributes to describe natural variability in mutualisms: the relative effect of trait matching on fitness, λ (equation 4 in the main text), and the number of mutualistic partners of individuals of species B, ω_B. In the following sections, we explore the model dynamics under alternative biological assumptions in relation to those we made when defining mutualism attributes in the main text.

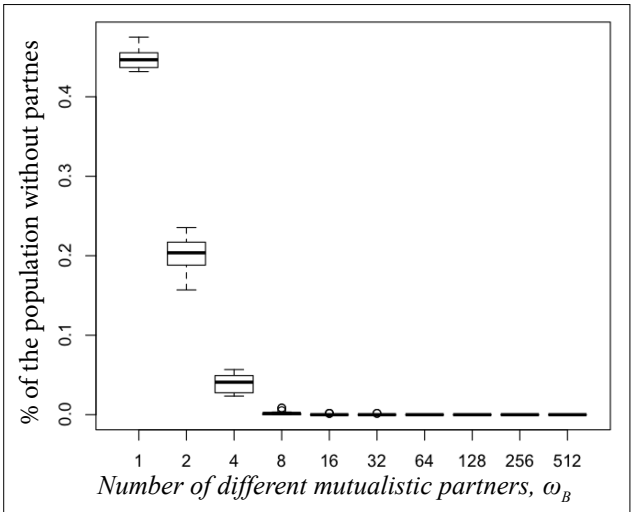

Figure A7. Percentage of the species A population remaining with no mutualistic partner within the first generation, under different numbers of mutualistic partners ω_B. Other parameters as in table A1s1**.**

Mutualism impact on the mating pool composition. In our model, species A is not limited regarding the number of interspecific partners individuals may have. Therefore, some individuals may interact much more times than others, whereas a proportion of the population may remain without mutualistic partners (fig. A7). The reproductive consequences for individuals remaining without any mutualistic partners could be: (i) reduced mating probabilities or (ii) preclusion from the mating pool. Indeed, highly intimate mutualisms can potentially filter individuals from the mating pool. We thus ran additional simulations in which we assumed that if individuals of species A were not selected by any mutualistic partner, they were also unable to mate ($P_{mat} = 0$). Adaptive diversification is constrained when highly intimate mutualisms ($\omega_B = \lambda = 1$) act as mating filters (see the main text for detailed results). The relative frequency of extreme phenotypes with relatively high mating probabilities decreases, since those individuals that suffered low intraspecific competition but did not interact are precluded from the mating pool.

Alternative P_{mut} computation. The fitness component describing the gain obtained by individuals from mutualistic interactions, P_{mut}, was computed by summing up the outcome of each interaction event. Although P_{mut} is a standardized fitness component (equation 4 in main text), we tested if the progressive limit imposed to diversification by increasing values of ω_B could simply be a consequence of the additive effect of interaction events. If P_{mut} is computed based on the mean benefit acquired by individuals, and is therefore proportional to mean trait complementarity, the effect of ω_B on adaptive diversification is consistent with the results of our simulation experiment (fig. A8).

Symmetric constrain on the number of individual mutualistic partners. In our simulation experiments, only species B individuals have a fixed number of mutualistic partners. However, we also explored an alternative scenario in which both species are constrained in relation to the number of partners with which individuals interact ($\omega_A = \omega_B$). We defined a preference vector with mutualistic partners for each individual of species B based on phenotype matching. Interaction occurred by rounds. In each round of interactions, the

order of individuals of species *B* choosing their preferred partner was randomly assigned. If a given individual of species *A* reached ω_A interactions, it was removed from the mutualistic partner pool available for species *B*. In this scenario, in which individuals of both species have limits to the number of interaction events, the degree of diversification also drops following the increase in the value of $\omega_A = \omega_B$ (fig. A9).

Relaxing the assumption of both species under disruptive selection

We explored the effect of relaxing the assumption that both species are under disruptive selection. We ran 20 replicates for each combination of ω_B (ω_B = 8, 64, 512) and λ values (λ = 0.1, 1) for cases in which (i) only species *A* is under disruptive selection, and (ii) only species *B* experiences the disruptive regime. Species richness is significantly lower (Tukey's HSD test, $Q = 2.34$, $p < 0.001$) in cases where species *A* ($S_A = 3.88 \pm 2.23$ spp. and SB = 4.00 ± 2.35 spp., $n = 120$ simulations) or species *B* ($S_A = 1.28 \pm 0.58$ spp. and $S_B = 1.19 \pm 0.41$ spp.,

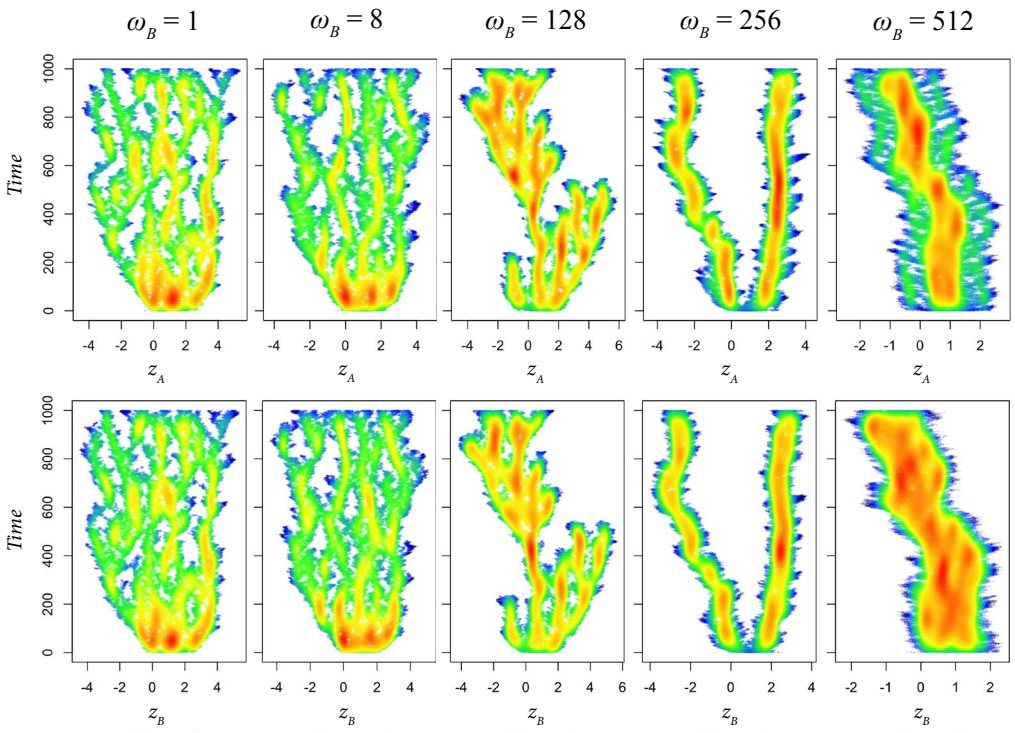

Figure A8. Individual-based simulations showing the effect of ω_B on adaptive diversification when the fitness component representing the gain acquired by individuals through mutualistic interactions, P_{mut}, is proportional to the mean trait complementarity of all interactions, instead of the sum of benefits obtained from each mutualistic partner (equation 3). Temperature colors represent density of individuals throughout the phenotypic space. Other parameters are the same as in table A1s1 with $N_A = N_B = 600$.

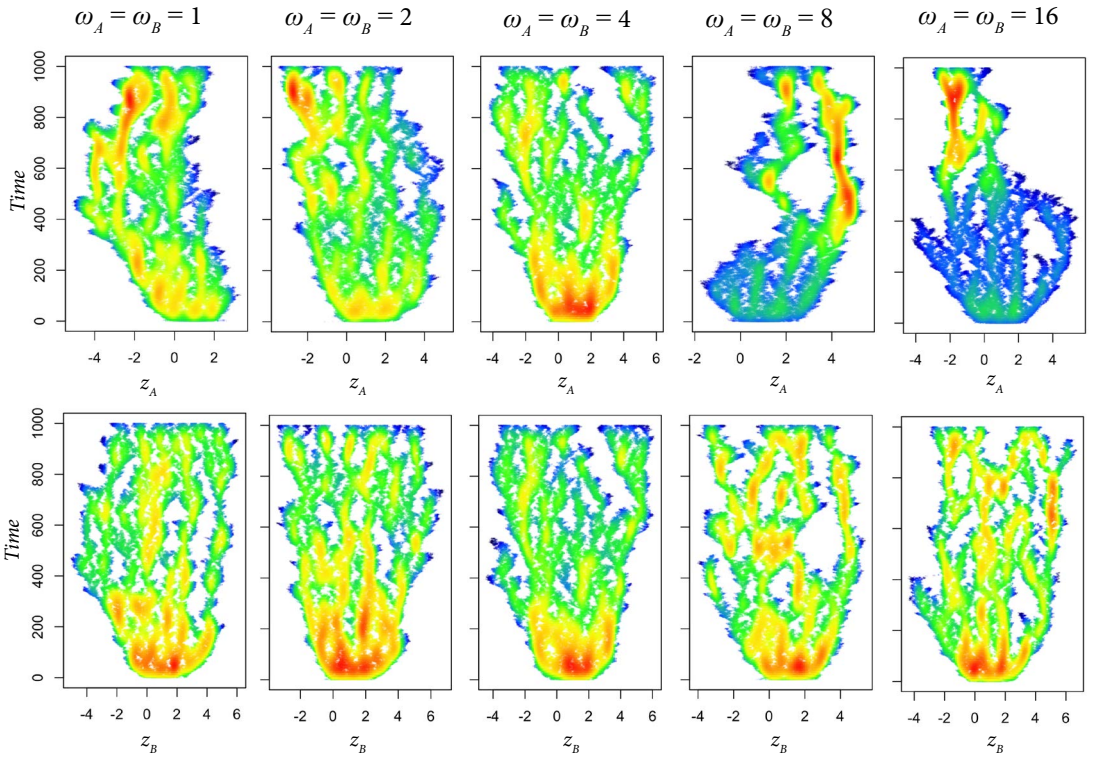

Figure A9. Adaptive diversification under increasing number of mutualistic partners per individual when both set of species have limits to the number of interaction events ($\omega_A = \omega_B$). Interactions occur by rounds. The order of individuals of species *B* choosing the partners is randomly assigned in each round. Each individuals interact ω_K times and than it is removed from the mutualistic pool. Colors represent individuals density. Other parameters are the same as in table A1s1 with $N_A = N_B = 600$.

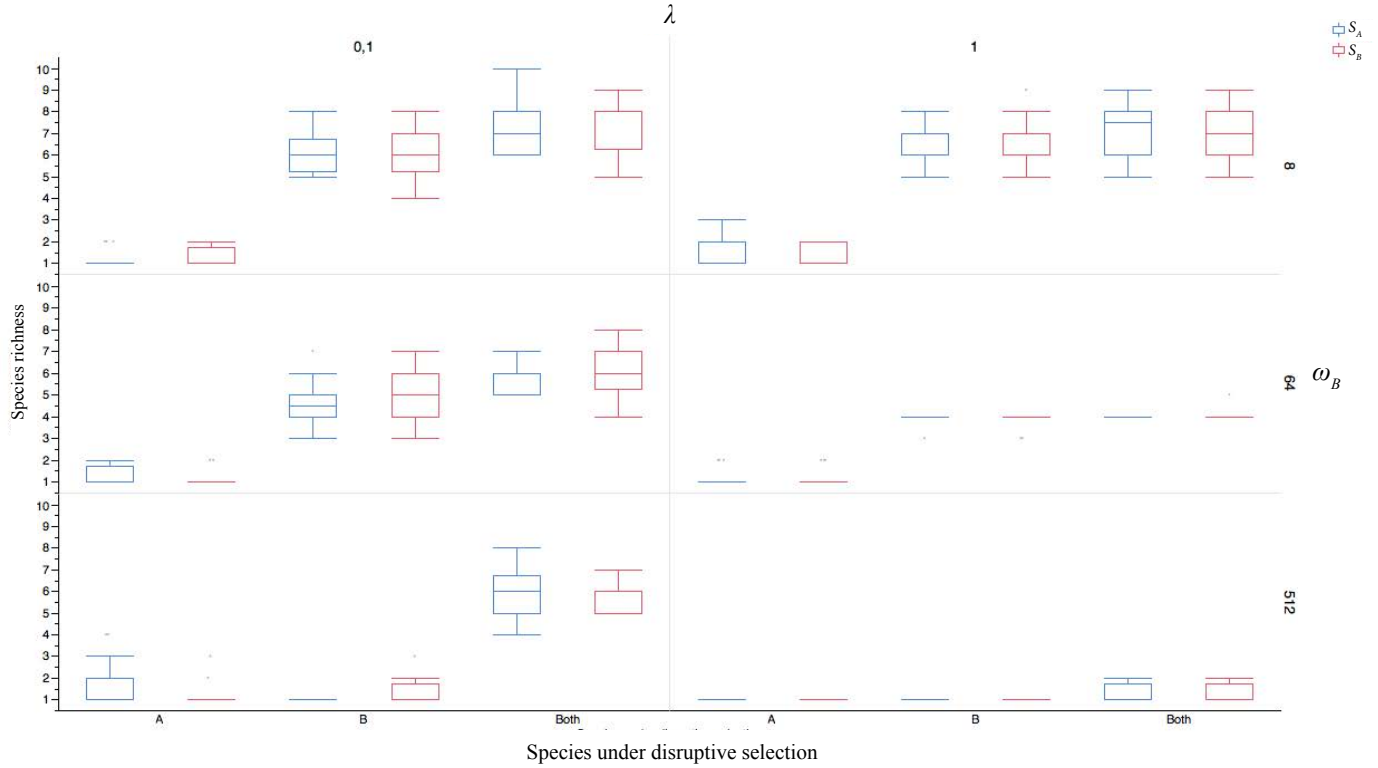

Figure A10. Asymptotic species richness for clades derived from species *A* (S_A) and from species *B* (S_B) when disruptive selection acts upon one of them (*A* or *B*) or both of them. Same parameters as in table A1s1 with $N = 600$.

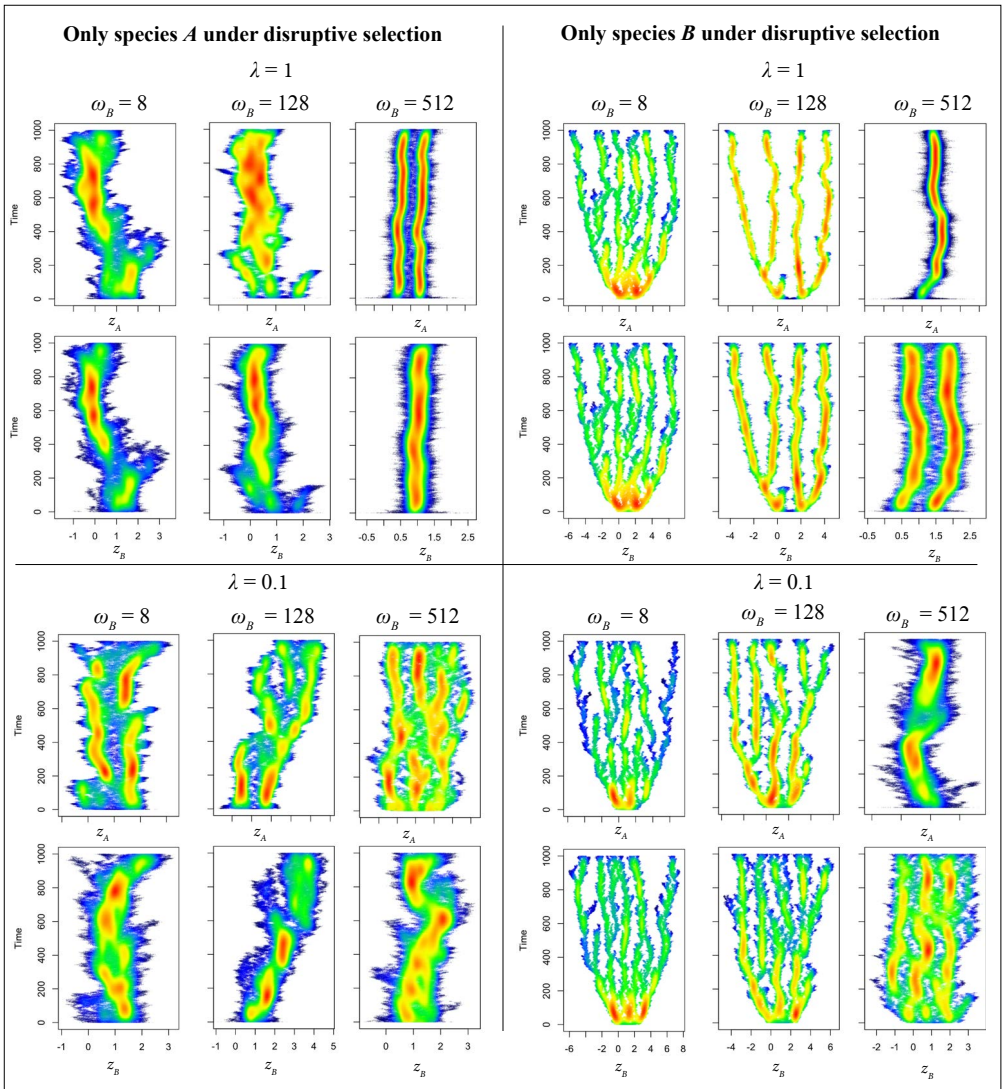

Figure A11. Phenotypic trajectories of traits z_A and z_B when only one of the species (A or B) is under disruptive selection. Same parameters as in table A1s1 with $N_A = N_B = 600$.

n = 120 simulations) are not subject to disruptive selection compared to the simulations in which both species experience a disruptive selective regime (S_A = 5.18 ± 2.23 spp. and S_B = 5.3 ± 2.3 spp., n = 120 simulations, fig. A10). Despite such quantitative differences, similar effects of ω_B and λ on diversification emerge if only species *B* faces disruptive selection. However, diversification is severely constrained if only species *A*, the one with individuals being chosen within the mutualistic interaction, experiences the disruptive regime. In this case, a low degree of diversification occurs when the effect of mutualistic trait matching on fitness decreases (fig. A11). These results show the degree of diversification achieved by *A* is highly dependent on the selective regimes operating in its mutualistic partner, *B*.

Relaxing the assumption of equal and constant population sizes

We relaxed the assumption that the overall number of individuals within each species or group of species is equal and constant over time. A first scenario of stochastic population dynamics, which is presented in the main text, assumes that each species' population varies randomly around a mean. At each generation, each species population size is defined by the initial population size ($N_A = N_B = 600$) summed to a parameter e whose value is sampled from a Gaussian with mean equal to zero and standard deviation $\sigma_{P(K)}$ (see the main text for details and results). In a second simulation, we allowed more drastic stochastic fluctuations of population sizes. Departing from initial population sizes of $N_{0(A)} = N_{0(B)} = 600$, the number of individuals $N_{t(K)}$ of a species/guild at the generation t is given by $N_{t-1(K)}$ +V, where V is a percentage of $N_{t-1(K)}$. At any given generation, V is randomly assigned to be positive or negative. We contrasted the diversification dynamics under different values of ω_B (8,32) and V (1%, 5%). In the resulting population dynamics, population sizes vary independently and can assume values much lower or much higher than the original sizes. Despite such a wide variation in population size, the general trend of decreased diversification following increasing ω_B is also observed (Figure A12). The trend is robust even for higher values of ω_B (64, 128) and V (10%, 15%) (results not shown).

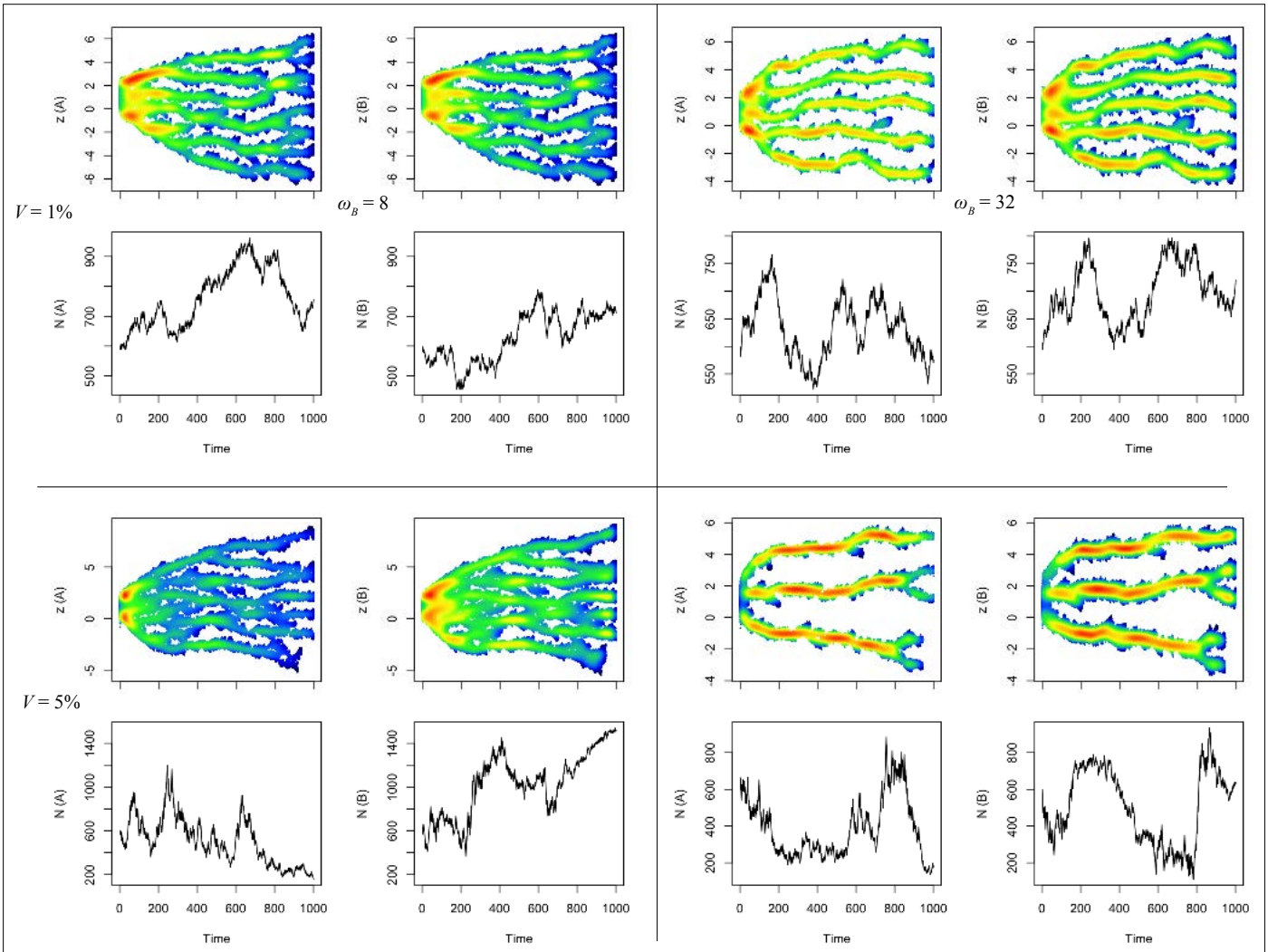

Figure A12. Phenotypic trajectories of traits z_A and z_B when population sizes vary stochastically. ω_B is the number of different mutualistic partners of each individual of species B. V is the parameter defining the degree of stochasticity to which the populations are subject. At any given generation, V is randomly assigned to be positive or negative. After that, a percentage V of the previous generation size is summed or subtracted to define the current generation size.

Literature cited in the Online Appendix

Carnell, Rob. 2009. Lhs: Latin Hypercube Samples. R package version 0.5.

Doebeli, M., and U. Dieckmann. 2000. Evolutionary branching and sympatric speciation caused by different types of ecological interactions. The American Naturalist 156: S77–S101.